Jurnal Teknologi, 56 (Sains & Kej.) Keluaran Khas (1), Dis. 2011: 27–52

EROSIVE WEAR OF NATURAL GAS PIPES DUE TO HIGH VELOCITY JET IMPACT: COMPUTER SIMULATION STUDY

Z. A. MAJID[1*], R. MOHSIN[2] & M. Z. YUSOF[3]

Abstract. A sequential failures of underground API 5L X42 carbon steel and the SDR 17, 125 mm polyethylene pipes placed side-by-side to a water pipe was studied. Previous study shown that high pressure water jet from leaked water pipe that had mixed with surrounding soil formed water soil slurry with high erosive properties had severely impacted on the pipe surface causing the loss of pipe coating materials. This phenomenon eventually causes rapid thinning of the steel pipe body which later led to its failure. In this study Computational Fluid Dynamics (CFD) and structural analysis were performed to simulate numerically the chronological event of pipeline failure, in comparison with the findings made in the previous study. The structural and CFD simulation results proved that the location, rate and the extent of erosion failures on the pipe surfaces can be well predicted, as compared with actual instances.

Keywords: Pipeline; natural gas pipe; slurry erosion; pipeline failure

1.0 INTRODUCTION

In tandem with the increasing demand of natural gas, more and more natural gas pipeline will be constructed. Natural gas pipeline system was designed and constructed in accordance to stringent standards. Various protective measures such as a warning tape, concrete slab as well as concrete marker were incorporated to the piping system to protect the pipes from any arising/possible dangers. Despite that a leak of these flammable gases is still unavoidable due to various factors such as corrosion, stress cracking, third party activities, and material defect.

[1&2] Gas Technology Centre, Universiti Teknologi Malaysia, 81310 UTM Johor Bahru, Johor , Malaysia
[3] School of Engineering, Universiti Tenaga Nasional 43000 Bangi Selangor, Malaysia
* Corresponding author: zulmajid@fkkksa.utm.my

A failure a natural gas piping system has been reported to be a major contributor for various explosion that involved losses of structures and lives as demonstrated in cases of pipe rupture in South Riding, Virginia in 1998 and Carlsbad, New Mexico in 2000 [1,2]. Statistically corrosion has been identified as major contributor for materials failure especially for underground piping system. Failure analysis on pipeline failures by Hasan *et al.* [3], C.R.F Azevedo [4], Shalaby *et al.* [5], Otegui *et al.* [6], and Kumar *et al.* [7] showed corrosion and stress cracking as a typical cause for the pipes to fail. There also a failure for natural gas pipe that caused by explosive as reported by Hasan [8].

Water jet is well applied in some industrial applications. It has been used intensively in abrasive water jet to cut metals for various industrial processes but uncontrolled water jet especially in erosive media such as in soil and sand could cause pipeline failure [9].

Erosion is define as an abrasive wear processes results by a repetitive impact of a solid particles entrained in a moving fluid against a surface causing a removal of material from that surface [10]. Bitter [11] defined erosion as "material damage caused by the attack of particles entrained in fluid stream system impacting the surface at high speed". Solid particle erosion or slurry erosion is a term to describe an effect of material removal by mean of particles impact in suspended fluid. It has been reported to be one source of a problem in many rotating equipment in various prime movers such as gas turbine, cyclone separators, boilers, and pump.

As corrosion has been recorded as main causes of pipeline failure, there is no or little attention given on the aspect of danger that could be created by the leaked adjacent water pipe to the gas pipe as a possible source of pipeline failure. Sand which normally used as part of backfilling material can form water sand slurry in the present of water. The impaction of this slurry has proven [9, 12-14] to causes metal loses and metal thinning in which eventually lead to pipeline failure. The 300mm separation distance between any utilities and gas pipe required by ASME B 31.8 is not suficient to retard this water sand slurry from reaching the pipe surface. As a results a natural gas pipes failure was reported after being buried only for six months in northern part of Malaysia [9].

Computer simulation is an effective method that complements the experimental techniques. It is a form of controlled computational experiments which allow various parameters to be studied separately under various conditions. In addition to that model generated by simulation process could gives

wider and better insight understanding of behavior of various engineering problems thus appropriate preventive measures can be designed accordingly. The use of this method by many researchers proven to shows good agreement with what was presented by analytical techniques [15-17]. A prediction of pipeline failure through computer simulation is proven to be effective methods to optimize the design of pipes and operating condition. Study by Yang *et al.* [17] on the failure analysis of a piping system in Hydroprocessing Reactor Effluent Air Cooler showed that the analytical results are in good agreement with the actual failure instances.

In this paper, erosive wear of API 5L X42 and SDR 17 125 mm polyethylene pipes are presented. A predictive methods using CFD modeling and structural analysis was employed to explain the erosion process of natural gas pipe (API 5L X42).

2.0 FLOW STUDY USING COMPUTATIONAL FLUID DYNAMICS (CFD)

In this study, the FLUENT software was used to simulate the sequence of processes that might have taken place which led to the failure of the gas pipes. The results obtained with the simulation try reinforce the hypothesis made in the earlier stage that the steel pipe leak was caused by the impaction of erosive soil water slurry from water pipe. As for the PE pipe, damages was then caused by the high pressure gas jet from the leak of the 1800 kPa (18 bar) 8 inch carbon steel pipe (API 5L X42). The objective of this analysis is to obtain the pressure and velocity profiles where the PE pipe was impinged by the gas jet stream. The information on how the gas jet flows from steel pipe behaved within the region is essential to strengthen the determination of the whole case study. The values obtained would also assist the structural simulation to model a more appropriate boundary condition.

2.1 Methodology

FLUENT 6 was chosen to assist the study due to its capabilities and validity. In order to model and study the problems through computing simulation, there were 3 sequences of activities that need to be executed accordingly as shown in Figure 1.

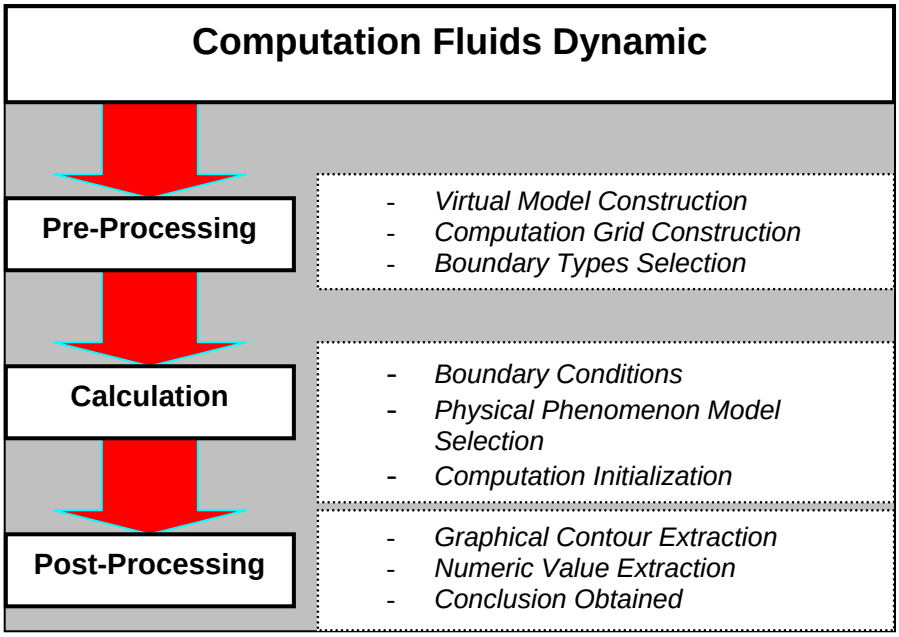

Figure 1 CFD methodology sequence

In the water jet simulation, the operating pressure was set to 10 bars at constant mode. No gas jet flow is involved since the primary intention of this part of the simulation is to obtain the flow behaviour on how the jet flow affects the steel pipe. As for the natural gas jet simulation, referring to the operating conditions involved, the problem can be classified as compressible flow type. Hence, heat energy coupled with flow energy model was used. Furthermore, in order to simplify the case study, only steady condition was applied. Under the steady condition, it was assumed that computational domain is fully immersed in homogeneous water distribution.

As for the working fluids, the properties water and methane were incorporated in the modeling. Methane which makes up more than 90% of the natural gas

composition is assumed to be representative of the natural gas properties. Gravitational effect must be included since the movements of water within the region are highly dependent or related to its body force as well. Water flow is not involved at this stage because after some time, certain equilibrium force between the domain which is flooded with water and water pipe flow will reach nearly equilibrium (region nearly saturated), water flow out from the pipe would decrease. Hence, in order to simplify the case study, water flow was assumed non exist.

Gas flow leak from PE pipe will not be studied as it was concluded that the PE pipe failed due to gas jet impingement from the steel pipe. Furthermore, due to the very high NPS8 gas jet pressure, the PE was expected to rupture very fast. The failure of the PE pipe should not affect other pipes. Jet flow produced by the PE pipe is considered weak due to the large failure outlet as shown in Figure 2.

Figure 2 Failed specimen of PE pipe

The pre-processing included physical modeling, setting-up appropriate boundary condition and construction of the computational mesh. Around 50,000 computational nodes (refer to Figure 3) were built and found to be sufficient in resolving computational domains. Boundary conditions that relate to geometric entities were set up for this particular work as shown in Table 1.

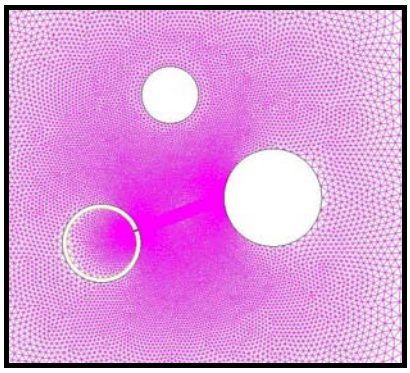

Water jet computational mesh

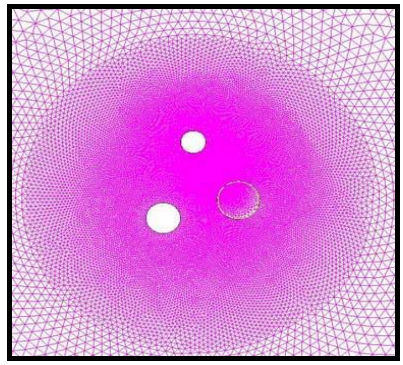

Natural gas jet computational mesh

Figure 3 Computational mesh for water jet and natural gas jet

Table1 List of boundary conditions

Boundary Type	Boundary Conditions	
	Steel Pipe Jet	**Asbestos Pipe Jet**
Pressure Inlet	Gas Inlet (18 Bar)	Water Inlet (10 Bar)
Pressure Outlet	Ambient (0 Bar)	Ambient (0 Bar)
Wall	Pipe Wall (Adiabatic)	Pipe Wall (Adiabatic)
Symmetry	Left, Right, Bottom Bound	Left, Right, Bottom Bound

2.2 Simulation Hypotheses

As the water pipe made of asbestos material, its brittle characteristic would cause the pipe to fail instantly. There will be no significant physical outlook left on the failed edge region. However, it was noticed from the photo taken from the site showing the upper part of the asbestos pipe seems experienced more failure than the lower part;

Figure 4 seems to support the hypothesis that the water jet direction is around 20° from the horizontal axis. The exact angle of 20° 29'of jet flow direction is determined through ideal geometrical approach by assuming the jet flow direction is normal to the surface of the outlet (normal impaction) as shown in Figure 5.

Exact initialization and condition of the asbestos pipe failure cannot be determined because the pipe was not made available to us and as seen in the picture, has already experienced major damage.

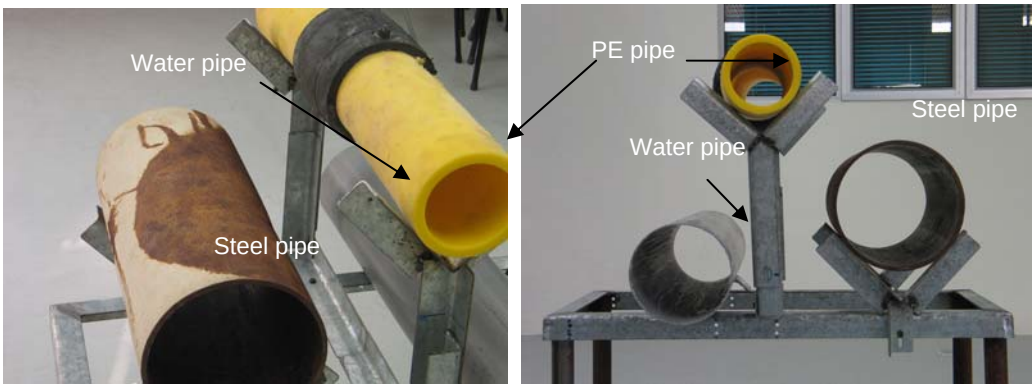

Figure 4 Reconstruction of relative pipe positions (original) for visual inspection

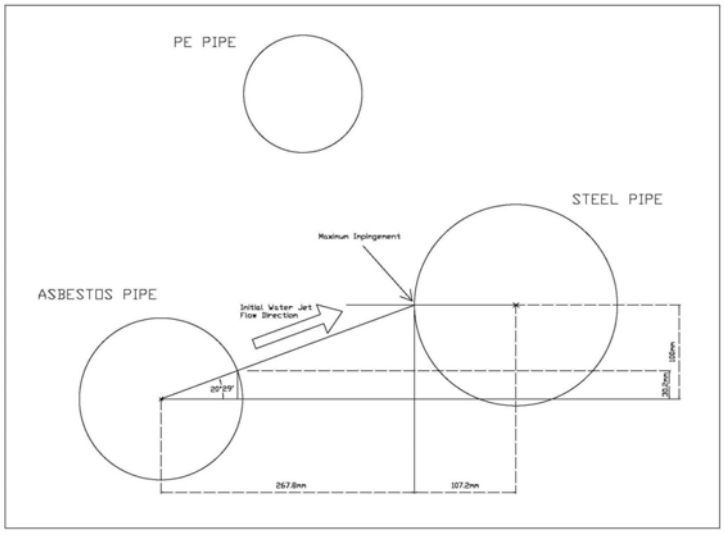

Figure 5 Water jet leak angle estimation

Reconstruction of the original position of pipes and insitu pipes position together with the recorded photos taken during the excavation of the failed site was able to deduce the following hypothesis:

i. PE pipe vertical position tends to be lowered (moving downward) due to
the lack of tangential support.

ii. As the medium is moving due to the jet flow from water pipe and steel pipe, PE pipe began to drop due the gravitational force and soil weight act on the PE pipe as shown in Figure 6.

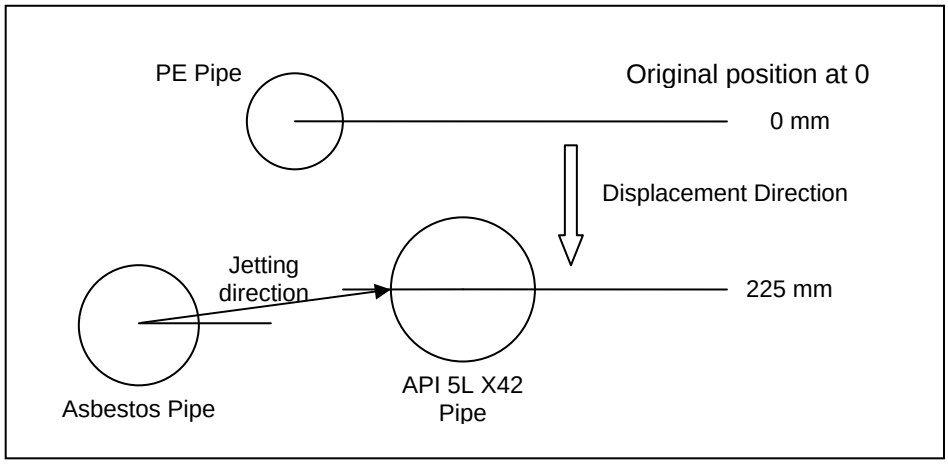

Figure 6 Schematic of PE pipeline displacement

iii. Water pipe (asbestos) and natural gas pipe (steel) is assumed not displaced due to its physical stiffness.

iv. Once the PE pipe began to displace, in-equilibrium force acting on the PE pipe will occur.

v. Expected operating strength of the PE pipe will reduce.

vi. From the existing design specification and sample of PE pipe, it was expected that the PE pipe would displace vertically around 225 mm away from the original position.

2.3 Simulation Results and Discussion of Water Pipe Leak

The results for the simulation of water pipe leak are given in Figures 7 and 8. The possible sequence of events are as follow:

i. Initially, the failure of the asbestos pipe would not create a big sized hole. Failure started as a small crack, possibly longitudinal in direction. The simulation was begun when the crack size has an effective diameter of 1.5 mm. The flow trajectory of the jet is as shown in Figures 7a and 8a.

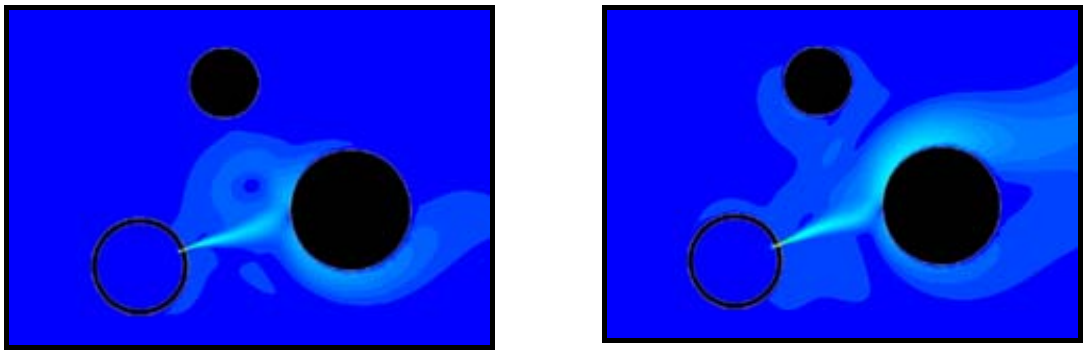

a. Hole size ≈ 1.5 mm b. Hole size ≈ 3.0 mm

Figure 7 Result of water jet simulation (2D velocity profile)

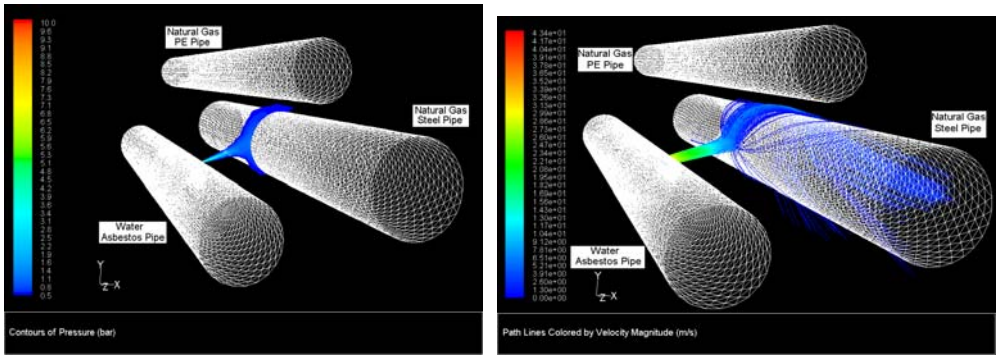

a. Hole size ≈ 1.5 mm b. Hole size ≈ 3.0 mm

Figure 8 Result of water jet simulation (3D velocity profile)

ii. As the effective diameter increased to 3.0 mm, it was shown that the force of the jet impacting on the steel pipe surface is getting much more significant (Figures 7b and 8b). It is believed the water

soil slurry is strong enough to cause coating losses on the steel pipe surface.

iii. The flow trajectory was also shown to mostly move along the upper surface of the steel pipe. This fact supports the finding of the surface profilometry study which shows a faster thinning process took place on the upper part of the pipe (previous study). This phenomenon totally agreed with the study conducted on cylindrical specimen using slurry pot erosion tester by H. McI. Clark [18]. This study reported that thinning behavior at centre and its surrounding of impaction for cylindrical ductile material is characterised by the cutting wear and deformation wear, respectively.

iv. The simulation results seem to agree with the observed conditions of the pipe surface conditions as shown in Figure 9.

Figure 9 Surface condition of API 5LX42 pipe

2.4 Simulation Results and Discussion of API 5L X42 Carbon Steel Pipe Leak

The results for the simulation of the API 5L X42 pipe leak in term of pressure and velocity contour are given in the picture sequence as in Figures 10 and 11 respectively.

The following are the discussion on the events that happened as the PE pipe moves downwards (Figure 6) due to the displacement and loss of supporting materials underneath it, as brought about by the continuous water and natural gas

jetting. These events have been derived from the CFD simulation results as depicted in Figures 10 and 11.

At 0 mm, 25 mm, 50 mm, 75 mm and 100 mm vertical displacement, the pressure contour shows that the pressure behaviour is not affected by the downward movement of the PE pipe. The velocity contour shows no significant difference. The jet flow from the steel pipe tends to flow and diffuse as expected.

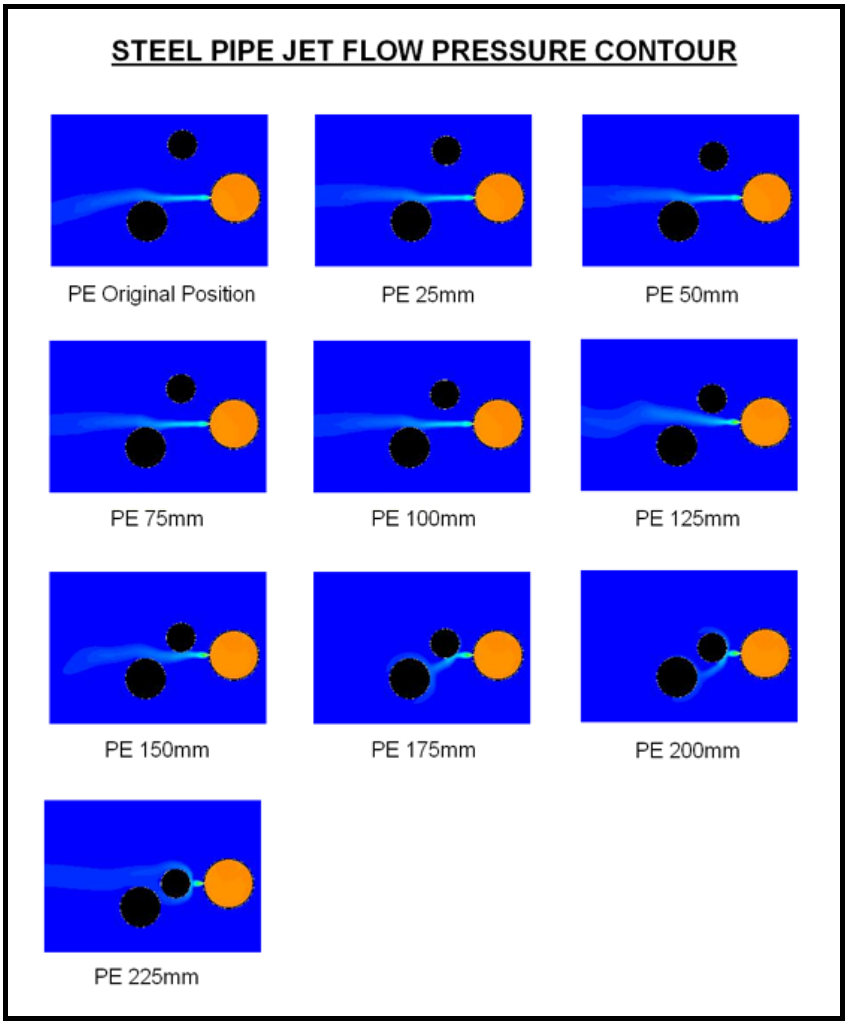

Figure 10 Gas pressure contours for the API 5L X42 pipe leak

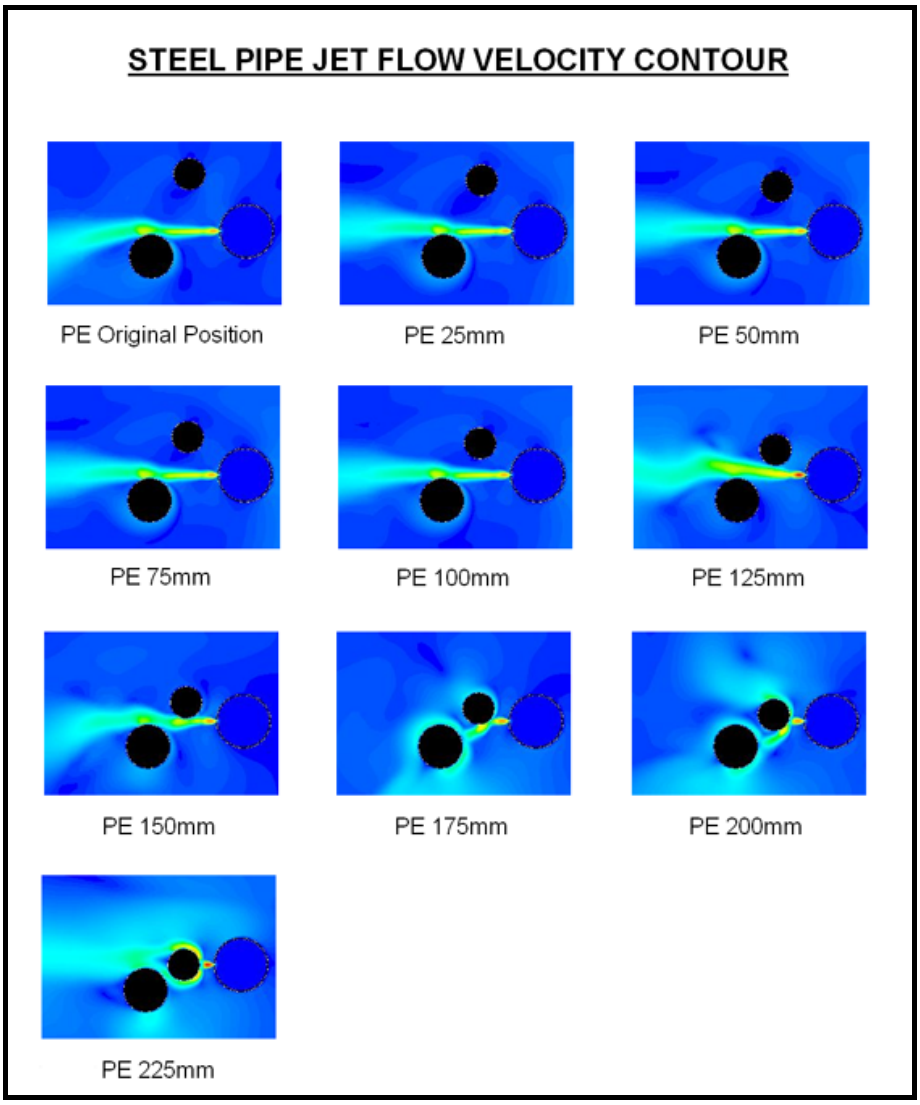

Figure 11 Gas flow velocity contours for the API 5L pipe leak

As the PE pipe was displaced around 125 mm, it was noticed that the pressure flow tend to change direction. This is due to the existing PE pipe near the flow region that cause external aerodynamic to occur. The upper side of the jet flow tends to move slower relative to the bottom side. Vorticity of flow will develop (Figure 12) due to the velocity difference between the two sides.

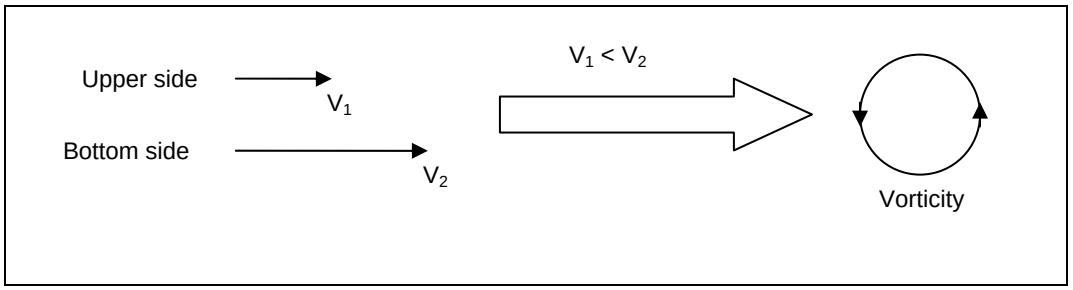

Figure 12 Vorticity flow development

This is due to the external shear force that was created at the upper side of the jet. The created shear force is due to the different media contact phenomenon. In fact, gravitational forces from the water also contribute to the situation. After certain distance, it was noticed that the flow began to move upward due to the lower natural gas specific gravity.

As the PE pipe dropped 150 mm, the gas jet hit the PE pipe. The PE pipe would start to shear by the gas jet flow. The pressure at this stage is around 1.7 bars and the flow velocity about 400 ms^{-1}. According to Figure 13, it is believed that the failure of PE pipe happened very fast.

Figure 13 On-site condition of damaged PE due to gas jet from API 5L X42 pipe

3.0 Structural Simulation Study Using Finite Element Analysis (FEA)

In this part of study, the NASTRAN software was used to simulate and evaluate the stresses that the steel pipe body faces especially in the vicinity of the failure region as the pipe thickness reduces due to the corrosion/erosion effect. This study will cover 3D and 2D failure studies with an aiming to identify the maximum stress and maximum displacement at the punch area. The 2D wall thickness reduction study was executed in order to understand the effect of pipe thickness reduction due to pipe erosion at failed area and to identify the pipe wall strength at minimal wall thickness as well as to identify the minimum wall thickness before rupture. Finally the pipe cross-section thickness mapping was studied to describe the thinning process that took place on the pipe outer surface and also from the wall thickness mapping, the thickness reduction occurs from the external corrosion effect.

3.1 Pipe Stress Fundamentals

3.1.1 Stress in Cylinder

The reactions in any cylinder develop both radial and tangential stresses with values, are dependant to the radius and wall thickness.

Tangential stress Radial stress

Figure 14 Stress profile in cylinder

Radial and tangential stresses are represented by the following formula:

$$\sigma_r = \frac{r_i^2 P_i}{r_o^2 - r_i^2} - \left(1 - \frac{r_o^2}{r^2}\right) \quad (1)$$

$$\sigma_t = \frac{r_i^2 P_i}{r_o^2 - r_i^2} - \left(1 + \frac{r_o^2}{r^2}\right) \quad (2)$$

Note: (+ve) Positive value indicate tension and (-ve) negative value indicate compression.

3.1.2 Thin Wall Vessel

If the wall thickness (t) of a cylindrical pressure vessel is about 1/20 or less of its radius (r), the radial stress which result in pressuring the vessels is relatively small compared tangential stress. Hence:

$$\sigma_{t,average} = \frac{P d_i}{2t} \quad (3)$$

$$\sigma_{t,maximum} = \frac{P(d_i + t)}{2t} \quad (4)$$

3.1.3 Von Mises Stress

Von Misses stress is used as a creation in determining the onset of failure in ductile materials. The failure creation states that the Von mises stress σ_{vm} should be less than the yield stress σ_v of the material. In the inequality form, the creation may be put as:

$$\sigma_{VM} \leq \sigma_Y \tag{5}$$

The Von Mises stress $\boldsymbol{\sigma_{vm}}$ is given by:

$$\sigma_{VM} = \sqrt{I_1^2 - 3I_2} \tag{6}$$

Where I_1 and I_2 are the first two invariants of the stress tensor. For the general state of stress given by Eq. 5 I_1 and I_2 are given by:

$$I_1 = \sigma_x + \sigma_y + \sigma_z \tag{7}$$

$$I_2 = \sigma_x\sigma_y + \sigma_y\sigma_z + \sigma_z\sigma_x - \tau_{yz}^2 - \tau_{xz}^2 - \tau_{xy}^2 \tag{8}$$

In term of the principal stresses $\boldsymbol{\sigma_1}$, $\boldsymbol{\sigma_2}$ and $\boldsymbol{\sigma_3}$, the two invariants can be written as:

$$I_1 = \sigma_1 + \sigma_2 + \sigma_3 \tag{9}$$

$$I_2 = \sigma_1\sigma_2 + \sigma_2\sigma_3 + \sigma_3\sigma_1 \tag{10}$$

It is easy to check that Von Misses given Eq. 1.45 can be expresses in the form:

$$\sigma_{VM} = \frac{1}{\sqrt{2}}\sqrt{(\sigma_1 - \sigma_2)^2 + (\sigma_2 - \sigma_3)^2 + (\sigma_3 - \sigma_2)^2} \tag{11}$$

For the state of plane stress, we have:

$$I_1 = \sigma_x + \sigma_y \tag{12}$$

$$I_2 = \sigma_x\sigma_y - \tau_{xy}^2 \tag{13}$$

And for plane strain:

$$\begin{aligned} I_1 &= \sigma_x + \sigma_y + \sigma_x \\ I_2 &= \sigma_x\sigma_y + \sigma_y\sigma_z + \sigma_z\sigma_x - \tau_{xy}^2 \end{aligned} \tag{14}$$

Where $\sigma_z = \nu(\sigma_x + \sigma_y)$

3.1.4 Wall Thickness Reduction Study

Assumed that original steel pipe thickness safety factor, n=42.

$$n_{pipe} = \frac{S_{material}}{\sigma_{permissible}} \tag{15}$$

By applying Von-misses theory,

$$\sigma_{VM} = \frac{1}{\sqrt{2}}\sqrt{(\sigma_1 - \sigma_2)^2 + (\sigma_2 - \sigma_3)^2 + (\sigma_3 - \sigma_2)^2} \tag{16}$$

$\sigma_1, \sigma_2, \sigma_3 =$ Normal stress obtain at critical location for each simulation

When the Von-misses stress values exceed the permissible stress, the structure (pipe) will fail.

3.2 Structural Geometry

In order to understand the real situation, the modeled geometry must be made as similar as possible to the real condition. Geometry for the pipe is developed using 3D Computer Aided Design (CAD) modeling by applying the following similarity factor:

i. Just a portion of the pipe being considered in order to reduce the meshing and analysis complexity. The pipe length used is 1000 mm (which is more than 20 diameter) where the effect or reaction at each end can be neglected;
ii. Carbon steel material is assumed homogeneous;
iii. The thickness of the pipe (API 5L X42) under consideration is assumed equal at any location which is 5.6 mm.

3.3 Results and Discussion of Fea Study

3.3.1 Stress Profile On Api5lx42 Pipe

Figure 15 shows the finite element simulation results. The summary of the results are tabulated in Table 1. The results show that as the punch depth gets deeper, the critical pressure due to the surface thickness reduction will increase. The critical element displacement also increased as the wall thickness is reduced. The pipe wall stress and displacement increase as a thickness of pipe reduce.

Case 1: Stress Profile	**Case 1: Displacement Profile**
Punch Depth: 0 mm (Pipe in normal operating condition) Punch Radius: 0 mm Internal pressure: 1.8 MPa Max displacement: $46.6X10^6$ Pa	Punch Depth: 0 mm (Pipe in normal operating condition) Punch Radius: mm Internal pressure: 1.8 MPa Max displacement: 0.0202 mm
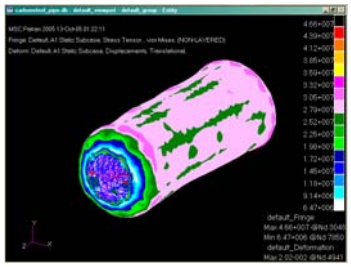	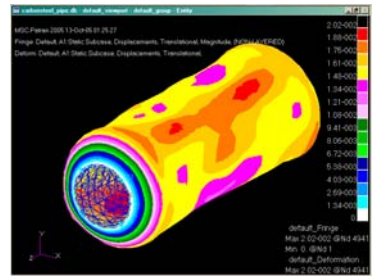
Case 2: Stress Profile	**Case 2: Displacement Profile**
Punch Depth: 2 mm Punch Radius: 1 mm Internal pressure: 1.8 MPa Max displacement: $47.4X10^6$ Pa	Punch Depth: 2 mm Punch Radius: 1 mm Internal pressure: 1.8 MPa Max displacement: 0.0206 mm
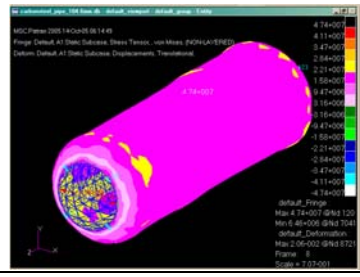	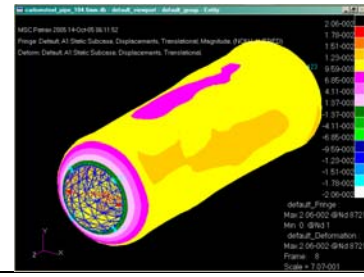

Figure 15 Stress profile on API 5L X42 pipe

Table 1 -D Simulation result summary

Case/ Punch	Pipe Thickness (mm)	Stress (MPa)	Displacement 10^{-2} (mm)
Normal	5.6	46.6	2.02
2mm	3.6	47.4	2.06
Hole	0	46.9	2.00

3.3.2 Wall Thickness Reduction Study

In the simulation, 1800 kPa internal pressure was applied from inside the pipe. Using the pipe dimension analysis (*thickness mapping*) the pipe thickness is modeled and simulated for different cases. The pipe thickness dimension model base is on the initial size which is 5.6 mm. The simulations were run for every 1mm reduction of pipe thickness as shown in Figure 16.

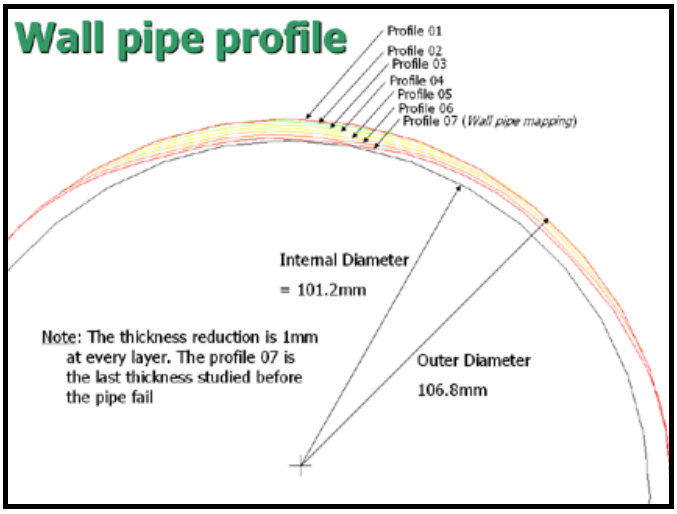

Figure 16 Steel pipe wall profile

The simulation results of 2D wall thickness reduction study are shown in Figure 17. The graphical representation of these results in term of graph of

maximum stress profile and maximum displacement are shown in Figures 18 and 19 respectively. These figures show that maximum stress a displacement increase in the similar pattern as the pipe become thinner.

Results for pipe wall profile 1	
Maximum stress results	**Displacement results**
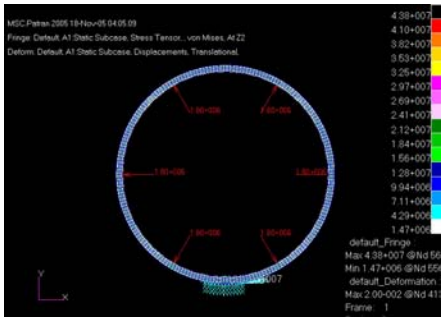	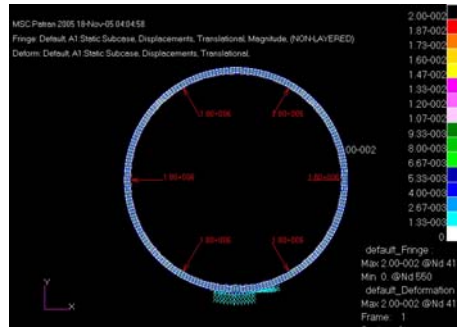
Results for pipe wall profile 4	
Maximum stress results	**Displacement results**
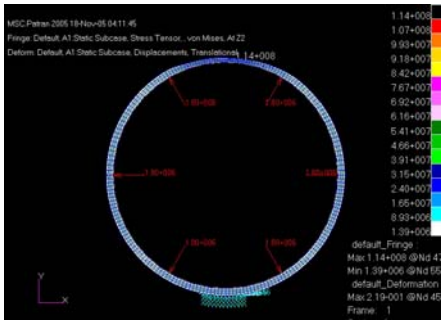	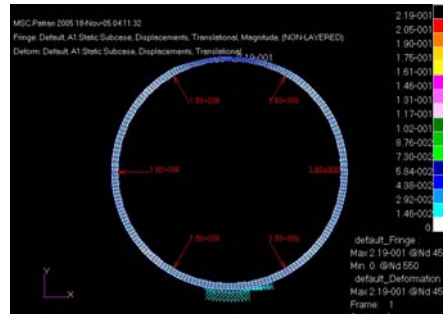
Results for pipe wall profile 7	
Maximum stress results	**Displacement results**
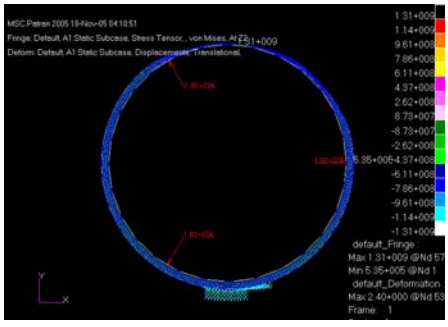	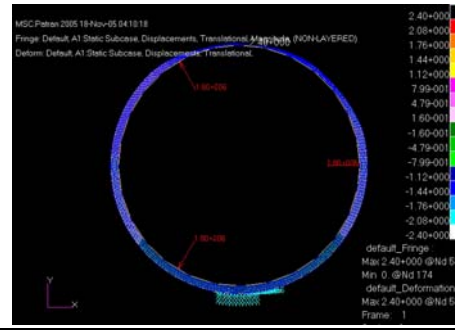

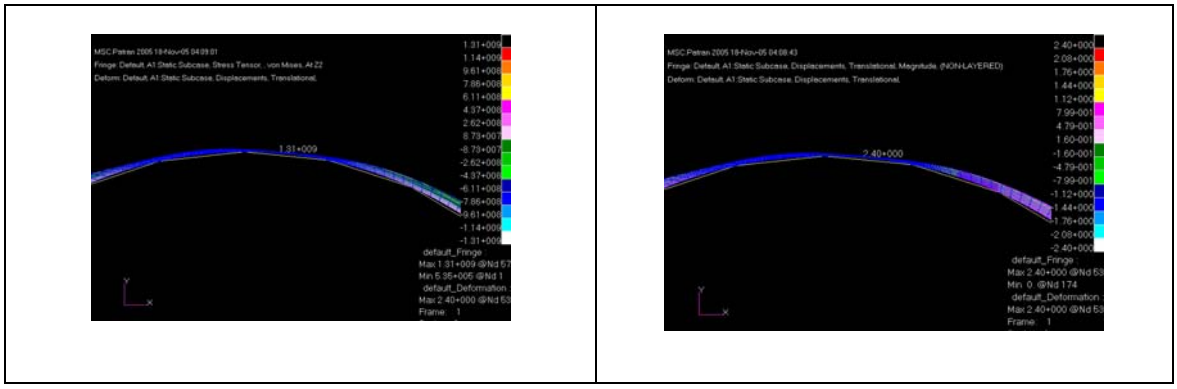

Figure 17 Max stress and displacement results at pipe wall

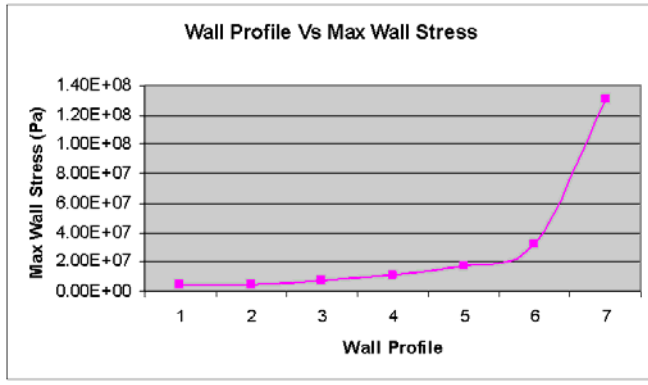

Figure 18 Maximum stress profile

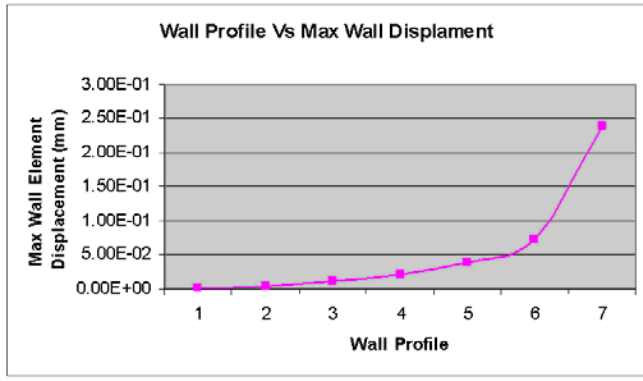

Figure 19 Maximum displacement profile

The tabulated results of thickness reduction and maximum stress (von-misses) and permissible stress on pipe wall is listed in Tables 3 and 4 respectively. A combination results for carbon steel pipe thinning behavior, showing relationship of pipe thickness reduction, Von-misses stress and operation safety (n) is in Figure 20.

After 4 mm (profile 5) surface thickness reduction the load (von-misses) exceed the permissible stress and lead to failure as indicated by n < 1. These results also indicated that if the wall thickness is lower than 1.5mm, the strength of the wall pipe is getting weaker and the minimum thickness before failure is lower than 1.25 mm.

Table 2 Results summary on the pipe wall stress profile

Simulation Job	Thickness reduction at the critical location (mm)	Von-Misses Stress (MPa)	n factor	Remarks
Profile 1	0.00	43.80	4.11	n>2
Profile 2	1.00	48.70	3.70	
Profile 3	2.00	76.30	2.36	n=2
Profile 4	3.00	114.00	1.58	
Profile 5	4.00	176.00	1.02	n=1
Profile 6	5.00	326.00	0.55	n<1
Profile 6.1	5.33	443.00	0.41	
Profile 6.2	5.67	666.00	0.27	
Profile 6.2.1	5.78	797.00	0.23	
Profile 6.2.2	5.89	988.00	0.18	
Profile 7	6.00	1310.00	0.14	

Note: n is the operating safety factor

Table 3 Results summary on the pipe wall stress profile

Profile	Stress (Pascal)		
	Max Stress (Von Misses)	Permissible Stress	Different
1	4.38E+06	9.30E+07	8.86E+07
2	4.87E+06	9.30E+07	8.81E+07
3	7.63E+06	9.30E+07	8.54E+07
4	1.14E+07	9.30E+07	8.16E+07
5	1.76E+07	9.30E+07	7.54E+07
6	3.26E+07	9.30E+07	6.04E+07
7	1.31E+08	9.30E+07	-3.80E+07

Note: red bolted number shows that the pipe has already failed when the maximum stress exceed the permissible stress

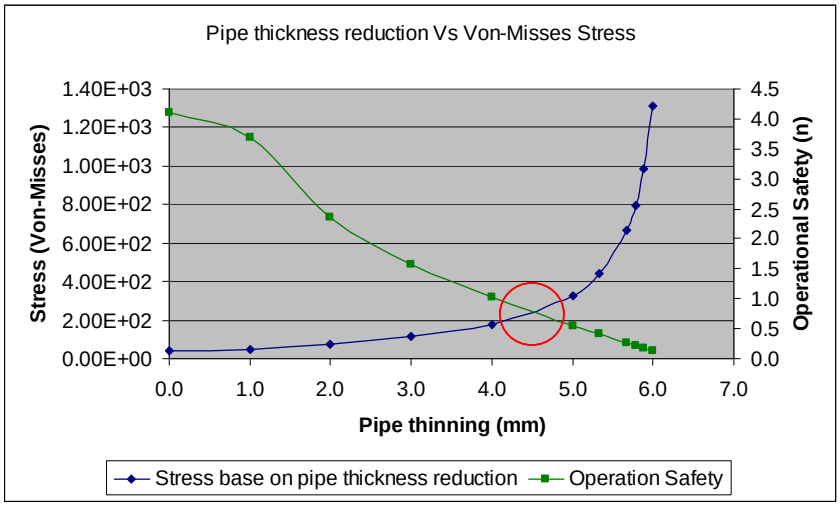

Figure 20 Combination results of carbon steel pipe thinning behaviour

3.4 Discussion on Structural Simulation Results

The investigation suggests that the asbestos water pipe with 10 mm wall thickness was the first to fail. It probably started with a small enough cracks that could have produce the strong jetting effect required to erode the steel pipe. The flowing water pressure in the pipe was reported to be 1000 kPa. The leak could have caused a high pressure water jet which, with the presence of the surrounding soil and sand materials, could have produced highly erosive slurry. This slurry could have impacted upon the API 5L X42, first causing the erosion of the coating materials and then the thinning of the steel pipe body. After sufficient pipe material was removed, the remaining pipe strength will no longer be able to withstand the high internal pipe pressure. This eventually led to the steel pipe pinhole rupture and eventual enlargement, forcing more gas out of the pipe.

The suggestion that the steel pipe developed the first leak and caused the damage of the water pipe can easily be refuted. Photo evidence (refer to Figure 21) the repositioning of the pipes showed that the steel pipe leak position is not directly facing the water pipe but rather towards the top. The opening of the water pipe that is directly facing the eroded part of the steel pipe.

Figure 21 Relative positions of the 8 inch water pipe to the NPS 8

The high pressure jet of leaked water from the 8 inch water pipe had earlier caused the displacement of the supporting soil materials underneath the PE 125 causing it to move downwards. When the steel gas pipe leaked, more materials was displaced causing the PE pipe to drop even further until it was low enough to be `*in the line of fire*' from the high pressure gas jet. It was estimated that the PE pipe dropped some 200 mm from its original position

4.0 CONCLUSIONS

The water jet will mix with soil to form water slurry with high erosive properties. It impacted upon the pipe surface causing the loss of pipe coating materials. Corrosion quickly ensued and material loss was rapid because of the continuous erosion of oxidised material that happened simultaneously. This phenomenon explains the rapid thinning of the steel pipe body which later led to its failure. Simulation results from both the CFD and structural study support these hypotheses as it matched the actual instances.

ACKNOWLEDGEMENT

Authors are most grateful and wish to all members of Gas Technology Center (GASTEG) Pipeline Failure Team for their significant efforts and commitments in conducting experiments and simulation throughout research period. Gas Malaysia Sdn. Bhd. (GMSB) is also highly acknowledged for providing pipe samples and continual financial support.

REFERENCES

[1] National Transportation Safety Board. 1998. Pipeline Incident Report, Natural Gas Pipeline Rupture and Fire in South Riding, Virginia, July 7 1998. Virginia: National Technical Information Service.

[2] National Transportation Safety Board. 2000. Pipeline Incident Report, Natural Gas Pipeline Rupture and Fire, Near Carlsbad, New Mexico, August 19 2000. Virginia: National Technical Information Service.

[3] F. Hassan, J. Iqbal, F. Ahmed. 2007. Stress Corrosion Failure of High-pressure Gas Pipeline. *Engineering Failure Analysis*. 14: 801-809.

[4] C. R. F. Azevedo. 2006. Failure Analysis of a Crude Oil Pipeline. *Engineering Failure Analysis*. 13: 789-796.

[5] H. M. Shalaby, W. T. Riad, A. A. Alhazza, M. H. Behbehani. 2006. Failure Analysis of Fuel Supply Pipeline. *Engineering Failure Analysis*. 13: 789-796.

[6] C. Manfredi, J. L. Otegui. 2002. Failures by SCC in Buried Pipelines. *Engineering Failure Analysis*. 9: 495-509.

[7] M. S. Kumar, M. Sujata, M. A. Venkataswamy, S. K. Bhaumik. 2008. Failures Analysis of Stainless Steel Pipeline. *Engineering Failure Analysis*. 15: 497-504

[8] F. Hassan, J. Iqbal. 2006. Consequential Rupture of Gas Pipeline. *Engineering Failure Analysis*. 13: 127-135.

[9] Z. A. Majid, R. Mohsin, Z. Yaacob, Z. Hassan. 2010. Failure Analysis of Natural Gas Pipes. *Eng Fail Anal*. 17: 818-37.

[10] I. M. Hutchings. 1974. Particle Erosion of Ductile Metals: A Mechanism of Material Removal. *Wear*. 27: 121-128.

[11] J. P. A. Bitter. 1963. A Study of Erosion Phenomena Part I. *Wear*. 6: 5.

[12] R. Hamzah, D. J. Stephenson, J. E. Strutt. 2004. Erosion of Materials used in Petroleum Production. *Wear*. 186: 493-496.

[13] F. Aimin, L. Jinming, T. Ziyun. 1995. Failure Analysis of the Impeller of Slurry Pump Subjected to Corrosive Wear. *Wear*. 181-182: 876-882.

[14] K. Haugen. O. Kvernvold, A. Ronold, R. Sandberg. 1995. Sand Erosive of Wear-resistance Materials: Erosion in Choke. *Wear*. 186-187: 179-188.

[15] M.S. ElTobgy, E. Ng, M.A. Elbestawi. 2005. Finite Element Modeling of Erosive Wear. *International Journal of Machine Tools & Manufacture*. 45: 1137-1346.

[16] Y. F. Wang, Z.G. Yang. 2008. Finite Element Model of Erosive Wear on Ductile and Brittle Materials. *Wear*. 265:871-878

[17] P. Tang, J. Yang, J. Zheng, I. Wong, S. He, J. Ye, G. Ou. 2009. Failure Analysis and Prediction of Pipes Due to the Interaction Between Multiphase Flow and Structure. Engineering Failure Analysis. 16: 1749-1756.

[18] H. McI. Clark. 1993. Specimen Diameter, Impact Velocity, Erosion Rate and Particle Density in a Slurry Pot Erosion Terster. *Wear*. 162-164: 669-678.

[19] I. Finnie. 1960. Erosion of Surfaces by Solid Particles. *Wear*. 3: 87.

[20] I. Finnie. 1972. Some Observation on the Erosion of Ductile Metals. *Wear*. 19: 81-90.

[21] J. P. A. Bitter. 1963. A Study of Erosion Phenomena Part II. *Wear*. 6: 169.

[22] J. H. Neilson, A. Gilchrist. 1967. Erosion by a Stream of Solid Particles. *Wear*. 11: 111-123.

[23] H. McI. Clark, K. K. Wong. 1995. Impact Angle, Particle Energy and Mass Loss in Erosion by Dilute Slurries.*Wear*. 186-187: 454-464.

[24] H. McI. Clark, R. B. Hartwich. 2001. A Re-Examination of the 'Particle Size Effect' in Slurry Erosion. *Wear*. 248: 147-161.